Chapter 2

Mathematical Models

The following sections present the equations which are used in the numerical simulations documented in this thesis. For clarity, equations have been presented in Cartesian tensor notation. Equivalent expressions for axisymmetric swirling flow and for a more general non-orthogonal coordinate system are provided in Appendices A and C.

2.1 Reynolds-Averaged Navier-Stokes Equations

The Reynolds-averaged expression for the conservation of mass, or as it is commonly termed the continuity equation, is expressed in Cartesian tensors as follows:

$$\frac{\partial \rho}{\partial t} + \frac{\partial}{\partial x_j}(\rho U_j) = 0 \tag{2.1}$$

where upper-case U_j is the mean velocity vector which has components (U,V,W) in the Cartesian (x,y,z) directions. Summation is implied by repeated indices and so the above expression can be expanded:

$$\frac{\partial \rho}{\partial t} + \frac{\partial}{\partial x}(\rho U) + \frac{\partial}{\partial y}(\rho V) + \frac{\partial}{\partial z}(\rho W) = 0 \tag{2.2}$$

Equation (2.1) can also be expanded, using the product rule:

$$\underbrace{\frac{\partial \rho}{\partial t}} + \rho\frac{\partial U_j}{\partial x_j} + \underbrace{U_j\frac{\partial \rho}{\partial x_j}} = 0 \tag{2.3}$$

For steady flows that do not involve compressibility effects, the two underbraced terms in the above expression are zero and continuity is written simply:

$$\frac{\partial U_j}{\partial x_j} = 0 \tag{2.4}$$

The above expression can also be employed for steady buoyancy-affected flows (provided they do not involve shock-waves) where it is assumed that density-gradients $(\partial\rho/\partial x_j)$ are small in comparison with strain-rates $(\partial U_j/\partial x_j)$.

The RANS equation for transport of momentum can be written in Cartesian tensors as follows:

$$\frac{\partial}{\partial t}(\rho U_i) + \frac{\partial}{\partial x_j}(\rho U_i U_j) = -\frac{\partial P}{\partial x_i} + \frac{\partial \tau_{ij}}{\partial x_j} \tag{2.5}$$

where P is the mean pressure and the stress tensor, τ_{ij}, is given by:

$$\tau_{ij} = \mu\left(\frac{\partial U_i}{\partial x_j} + \frac{\partial U_j}{\partial x_i} - \underbrace{\frac{2}{3}\delta_{ij}\frac{\partial U_k}{\partial x_k}}\right) - \rho\overline{u_i u_j} \tag{2.6}$$

The term $\overline{u_i u_j}$ is the Reynolds stress tensor and δ_{ij} the Kronecker delta which is zero if $i \neq j$ and unity if $i = j$. The underbraced term in Equation (2.6) makes the trace[1] of the viscous stress tensor zero. In its most general form, the Boussinesq Eddy-Viscosity Model (EVM) can be written in Cartesian tensors:

$$-\rho\overline{u_i u_j} = \mu_t\left(\frac{\partial U_i}{\partial x_j} + \frac{\partial U_j}{\partial x_i} - \underbrace{\frac{2}{3}\delta_{ij}\frac{\partial U_k}{\partial x_k}}\right) - \underbrace{\frac{2}{3}\delta_{ij}\rho k} \tag{2.8}$$

where k is the turbulent kinetic energy and the two underbraced terms are included to satisfy the trace condition, $\overline{u_i u_i} = 2k$.

2.2 Linear $k-\varepsilon$ Model

In the low-Reynolds-number linear $k-\varepsilon$ model of Launder & Sharma, the eddy-viscosity is calculated from:

$$\mu_t = \rho c_\mu f_\mu \frac{k^2}{\tilde{\varepsilon}} \tag{2.9}$$

where c_μ is assumed constant $(c_\mu = 0.09)$, the damping function f_μ is given by:

$$f_\mu = \exp\left[\frac{-3.4}{\left(1+\tilde{R}_t/50\right)^2}\right] \tag{2.10}$$

[1]The trace of the expression is obtained by setting $i = j$ and summing over repeated indices. The trace of the viscous part of the stress tensor is given by:

$$\mu\left(\frac{\partial U_i}{\partial x_i} + \frac{\partial U_i}{\partial x_i} - 2\frac{\partial U_k}{\partial x_k}\right) = 0 \tag{2.7}$$

Tensors with zero trace are also called “deviatoric”. If the flow is incompressible the underbraced term in Equation (2.6) is zero.

and the turbulence Reynolds number, $\tilde{R}_t$, is defined by:

$$\tilde{R}_t = \frac{k^{1/2} l}{\nu} = \frac{k^2}{\nu \tilde{\varepsilon}} \tag{2.11}$$

The function f_μ accounts for both the true viscous damping at low Reynolds number and the preferential damping of the wall-normal fluctuations as the wall is approached.

Transport equations are solved for the turbulent kinetic energy, k, and isotropic dissipation rate, $\tilde{\varepsilon}$. The exact transport equation for k can be derived from its definition $(k = \overline{u_i u_i}/2)$, using the transport equation for the Reynolds stress tensor, $\overline{u_i u_j}$ and approximating diffusion terms in the resulting expression by an eddy-diffusivity model. This gives the following expression:

$$\frac{\partial}{\partial t}(\rho k) + \frac{\partial}{\partial x_j}(\rho U_j k) = \frac{\partial}{\partial x_j}\left[\left(\mu + \frac{\mu_t}{\sigma_k}\right)\frac{\partial k}{\partial x_j}\right] + P_k - \rho\varepsilon \tag{2.12}$$

The terms on the left-hand side represent convection and those on the right are diffusion, production and dissipation, respectively (reading left to right). The constant σ_k is the effective Prandtl number for the diffusion of kinetic energy (taken as $\sigma_k = 1.0$ in the Launder-Sharma model) and the production rate of kinetic energy, P_k, is calculated from:

$$P_k = -\rho\overline{u_i u_j}\frac{\partial U_i}{\partial x_j} \tag{2.13}$$

Unlike turbulent kinetic energy, the dissipation rate does not fall to zero at the wall. Instead ε takes a value at the wall which balances the rate of diffusion of turbulent kinetic energy towards the wall (as discussed in Section 1.3). For numerical convenience, rather than solve an equation for ε, a transport equation is solved for the isotropic dissipation rate $(\tilde{\varepsilon})$ which, by definition, falls to zero on the wall surface (see Jones & Launder [12]). The dissipation rate term appearing in the k-equation is the total dissipation rate, defined as:

$$\varepsilon = \tilde{\varepsilon} + 2\nu\left(\frac{\partial k^{1/2}}{\partial x_j}\right)^2 \tag{2.14}$$

The modelled equation for the isotropic dissipation rate follows a similar format to the k-equation, being composed of convection, diffusion, production and dissipation components:

$$\frac{\partial}{\partial t}(\rho\tilde{\varepsilon}) + \frac{\partial}{\partial x_j}(\rho U_j \tilde{\varepsilon}) = \frac{\partial}{\partial x_j}\left[\left(\mu + \frac{\mu_t}{\sigma_\varepsilon}\right)\frac{\partial \tilde{\varepsilon}}{\partial x_j}\right] + c_{\varepsilon 1} f_1 P_k \frac{\tilde{\varepsilon}}{k} - c_{\varepsilon 2} f_2 \rho \frac{\tilde{\varepsilon}^2}{k} + \rho Y_c + P_{\varepsilon 3} \tag{2.15}$$

The final two terms on the right-hand-side of the above equation are the Yap correction, Y_c, and a low-Reynolds-number turbulence damping term, $P_{\varepsilon 3}$ (sometimes denoted E). The Yap correction [64] is used to reduce the departure of the turbulence length scale $\left(l = k^{3/2}/\varepsilon\right)$ from the local equilibrium length scale $(l_e = 2.55y)$. It was developed initially in response to studies of impinging jets and pipe expansions that showed that the linear $k-\varepsilon$ model overpredicted heat transfer near the stagnation and

reattachment points (see, for example, [65]). The standard Yap correction is given by:

$$Y_c = \max\left\{\left[0.83\left(\frac{k^{3/2}/\tilde{\varepsilon}}{2.55y}-1\right)\left(\frac{k^{3/2}/\tilde{\varepsilon}}{2.55y}\right)^2\frac{\tilde{\varepsilon}^2}{k}\right],0\right\} \tag{2.16}$$

where y is the wall-normal distance. The above expression can introduce problems in certain flows with complex geometry where it is difficult to define a wall-normal distance. For this reason, Iacovides & Raisee [66] introduced an alternative correction based on the gradient of the length scale (a so-called differential Yap correction, Y_{dc}) which is independent of wall distance. This takes the following form:

$$Y_{dc} = c_w\frac{\tilde{\varepsilon}^2}{k}\max\left[F\left(F+1\right)^2,0\right] \tag{2.17}$$

where:

$$F = \frac{1}{c_l}\left[\left(\frac{\partial l}{\partial x_j}\frac{\partial l}{\partial x_j}\right)^{1/2} - dl_e dy\right] \tag{2.18}$$

$$dl_e dy = c_l\left[1-\exp\left(-B_\varepsilon\tilde{R}_t\right)\right] + B_\varepsilon c_l\tilde{R}_t\exp\left(-B_\varepsilon\tilde{R}_t\right) \tag{2.19}$$

c_l	B_ε	c_w
2.55	0.1069	0.83

The c_w constant was later modified by Craft *et al*. [67] to reduce the degree of correction in regions of high straining and to improve numerical stability. In this more recent form, c_w is made a function of the strain-rate and vorticity invariants and turbulence Reynolds number, as follows:

$$c_w = \frac{0.83\min(1,\tilde{R}_t/5)}{\left[0.8+0.7\left(\eta'/3.33\right)^4\exp(-\tilde{R}_t/12.5)\right]} \tag{2.20}$$

where:

$$\eta' = \max\left(\tilde{S}',\tilde{\Omega}'\right) \tag{2.21}$$

$$\tilde{S}' = \max\left(\frac{k}{\tilde{\varepsilon}},\sqrt{\frac{\nu}{\varepsilon}}\right)\sqrt{\frac{1}{2}S_{ij}S_{ij}} \tag{2.22}$$

$$\tilde{\Omega}' = \max\left(\frac{k}{\tilde{\varepsilon}},\sqrt{\frac{\nu}{\varepsilon}}\right)\sqrt{\frac{1}{2}\Omega_{ij}\Omega_{ij}} \tag{2.23}$$

The effect of the Yap correction is far greater with low-Reynolds-number formulations than with standard wall functions formulations, but the effect is still measurable with the latter (see discussion in Chapter 5, in particular Figures 5.31 and 5.32). Both "standard" and differential Yap corrections are tested in this thesis, the latter using the variable c_w of Craft *et al*. (Equation 2.20).

The gradient production source term, $P_{\varepsilon 3}$, is included in the $\tilde{\varepsilon}$-equation to obtain the correct near-wall distribution of k [12]. The expression for $P_{\varepsilon 3}$ and the remaining constants and damping functions

used in the $\tilde{\varepsilon}$-equation are as follows:

$$P_{\varepsilon 3} = 2\mu\nu_t \left(\frac{\partial^2 U_i}{\partial x_j \partial x_k} \right)^2 \tag{2.24}$$

$$f_1 = 1.0 \tag{2.25}$$

$$f_2 = 1.0 - 0.3\exp\left(\tilde{R}_t^2\right) \tag{2.26}$$

$c_{\varepsilon 1}$	$c_{\varepsilon 2}$	σ_ε
1.44	1.92	1.3

2.3 Non-Linear $k-\varepsilon$ Model

In the non-linear eddy-viscosity model (NLEVM) of Craft *et al*. [30], additional quadratic and cubic functions of strain and vorticity are introduced into the equation for the Reynolds stress. The constitutive equation for the Reynolds stress anisotropy, a_{ij}, defined as the ratio of the deviatoric Reynolds stress to the turbulent kinetic energy, is as follows:

$$\begin{aligned} a_{ij} \equiv \frac{\overline{u_i u_j}}{k} - \frac{2}{3}\delta_{ij} &= -\frac{\nu_t}{k} S_{ij} \\ &\quad + c_1 \frac{\nu_t}{\tilde{\varepsilon}} \left(S_{ik}S_{kj} - \frac{1}{3} S_{kl}S_{kl}\delta_{ij} \right) \\ &\quad + c_2 \frac{\nu_t}{\tilde{\varepsilon}} \left(\Omega_{ik}S_{kj} + \Omega_{jk}S_{ki} \right) \\ &\quad + c_3 \frac{\nu_t}{\tilde{\varepsilon}} \left(\Omega_{ik}\Omega_{jk} - \frac{1}{3}\Omega_{lk}\Omega_{lk}\delta_{ij} \right) \\ &\quad + c_4 \frac{\nu_t k}{\tilde{\varepsilon}^2} \left(S_{ki}\Omega_{lj} + S_{kj}\Omega_{li} \right) S_{kl} \\ &\quad + c_5 \frac{\nu_t k}{\tilde{\varepsilon}^2} \left(\Omega_{il}\Omega_{lm}S_{mj} + S_{il}\Omega_{lm}\Omega_{mj} - \frac{2}{3} S_{lm}\Omega_{mn}\Omega_{nl}\delta_{ij} \right) \\ &\quad + c_6 \frac{\nu_t k}{\tilde{\varepsilon}^2} S_{ij}S_{kl}S_{kl} \\ &\quad + c_7 \frac{\nu_t k}{\tilde{\varepsilon}^2} S_{ij}\Omega_{kl}\Omega_{kl} \end{aligned} \tag{2.27}$$

where the strain-rate and vorticity tensors are given by:

$$S_{ij} = \frac{\partial U_i}{\partial x_j} + \frac{\partial U_j}{\partial x_i} \qquad \Omega_{ij} = \frac{\partial U_i}{\partial x_j} - \frac{\partial U_j}{\partial x_i} \tag{2.28}$$

Quadratic combinations of S and Ω are necessary in order to capture the Reynolds stress anisotropy in simple shear flows, whilst cubic terms are necessary to correct for streamline curvature and swirl (for details see [34]).

The eddy-viscosity is calculated as previously in the linear EVM:

$$\nu_t = c_\mu f_\mu \frac{k^2}{\tilde{\varepsilon}} \tag{2.29}$$

and the near-wall damping function, f_μ, and the $\tilde{\varepsilon}$-equation source term, $P_{\varepsilon 3}$, are re-optimized:

$$f_\mu = 1 - \exp\left[\left(-\frac{\tilde{R}_t}{90}\right)^{1/2} - \left(-\frac{\tilde{R}_t}{400}\right)^2\right] \tag{2.30}$$

$$\begin{aligned} P_{\varepsilon 3} &= 0.0022\frac{\tilde{S}\mu_t k^2}{\tilde{\varepsilon}}\left(\frac{\partial^2 U_i}{\partial x_j \partial x_k}\right)^2 \quad \text{for} \quad \tilde{R}_t \leq 250 \\ &= 0 \qquad\qquad\qquad\qquad\qquad\quad \text{for} \quad \tilde{R}_t > 250 \end{aligned} \tag{2.31}$$

where $\tilde{S}$ is the dimensionless strain invariant, calculated from:

$$\tilde{S} = \frac{k}{\tilde{\varepsilon}}\sqrt{\frac{1}{2}S_{ij}S_{ij}} \tag{2.32}$$

The constant value of c_μ used in the Launder & Sharma $k-\varepsilon$ model was derived by considering simple shear flows where production and dissipation of turbulence energy are in balance and hence the ratio of shear stress to kinetic energy is approximately constant ($c_\mu = (\overline{uv}/k)^2 \approx 0.09$). In the Craft *et al*. model, c_μ is made a function of the strain-rate and vorticity invariants. The original formulation for c_μ, developed by Suga [34], is as follows:

$$c_\mu = \min\left(0.09, \frac{0.3}{1+0.35\eta^{1.5}}\left\{1-\exp\left[-0.36\exp\left(0.75\eta\right)\right]\right\}\right) \tag{2.33}$$

where:

$$\eta = \max\left(\tilde{S}, \tilde{\Omega}\right) \tag{2.34}$$

and the dimensionless vorticity invariant, $\tilde{\Omega}$, is given by:

$$\tilde{\Omega} = \frac{k}{\tilde{\varepsilon}}\sqrt{\frac{1}{2}\Omega_{ij}\Omega_{ij}} \tag{2.35}$$

More recently, Craft *et al*. [67] introduced a c_μ function with a slightly weaker dependence on the strain and vorticity invariants which was found to suffer less from unstable feedback[2]:

$$c_\mu = \min\left(0.09, \frac{1.2}{1+3.5\eta+f_{RS}}\right) \tag{2.36}$$

with:

$$f_{RS} = 0.235\left[\max\left(0, \eta - 3.333\right)\right]^2\left[\exp\left(-\tilde{R}_t/400\right) + \sqrt{S_I^2}\right] \tag{2.37}$$

where the third invariant of the strain-rate tensor, S_I, is given by:

$$S_I = \frac{S_{ij}S_{jk}S_{ki}}{\left(S_{nl}S_{nl}/2\right)^{3/2}} \tag{2.38}$$

[2] As discussed in Craft *et al*. [67], a c_μ function based on strain and vorticity invariants can lead to numerical instabilities where an overpredicted strain-rate leads to a reduced c_μ, which in turn reduces the eddy-viscosity and leads to an increased strain-rate, which then reduces c_μ etc.

Both of the above c_μ functions have been tested in this thesis. The recent Craft *et al*. paper also described a number of methods for improving the stability of the NLEVM. The last two cubic terms in the NLEVM expression, Equation (2.27), with coefficients c_6 and c_7 are tensorially linear, being composed of a product of the strain-rate, S_{ij}, and a scalar parameter. The linear term and these two cubic terms can thus be combined as follows:

$$\begin{aligned} a_{ij} \equiv \frac{\overline{u_i u_j}}{k} - \frac{2}{3}\delta_{ij} = \; & - \left(\frac{\nu_t}{k} - c_6 \frac{\nu_t k}{\tilde{\varepsilon}^2} S_{kl} S_{kl} - c_7 \frac{\nu_t k}{\tilde{\varepsilon}^2} \Omega_{kl} \Omega_{kl} \right) S_{ij} \\ & + c_1 \frac{\nu_t}{\tilde{\varepsilon}} \left(S_{ik} S_{kj} - \frac{1}{3} S_{kl} S_{kl} \delta_{ij} \right) \\ & + c_2 \frac{\nu_t}{\tilde{\varepsilon}} \left(\Omega_{ik} S_{kj} + \Omega_{jk} S_{ki} \right) \\ & + c_3 \frac{\nu_t}{\tilde{\varepsilon}} \left(\Omega_{ik} \Omega_{jk} - \frac{1}{3} \Omega_{lk} \Omega_{lk} \delta_{ij} \right) \\ & + c_4 \frac{\nu_t k}{\tilde{\varepsilon}^2} \left(S_{ki} \Omega_{lj} + S_{kj} \Omega_{li} \right) S_{kl} \\ & + c_5 \frac{\nu_t k}{\tilde{\varepsilon}^2} \left(\Omega_{il} \Omega_{lm} S_{mj} + S_{il} \Omega_{lm} \Omega_{mj} - \frac{2}{3} S_{lm} \Omega_{mn} \Omega_{nl} \delta_{ij} \right) \end{aligned} \tag{2.39}$$

When the sum of the c_6 and c_7 terms in the first line of Equation (2.39) is negative, their contribution to the coefficient of S_{ij} will be positive, in effect increasing the magnitude of the eddy-viscosity, which improves numerical stability. The momentum equation can therefore be rewritten, following the same sign convention used in Craft *et al*. [67]:

$$\rho U_j \frac{\partial U_i}{\partial x_j} = \frac{\partial P}{\partial x_i} + \frac{\partial}{\partial x_j} \left(\left(\mu + \mu_t' \right) S_{ij} - \rho \widehat{\overline{u_i u_j}} \right) \tag{2.40}$$

where the modified eddy-viscosity, μ_t', includes any positive contribution from the last two cubic terms in Equation (2.27), and $\widehat{\overline{u_i u_j}}$ contains the remaining higher-order components of the Reynolds stress, i.e.:

$$\mu_t' = \mu_t - \mu_t \frac{k^2}{\tilde{\varepsilon}^2} \min \left[\left(c_6 S_{kl} S_{kl} + c_7 \Omega_{kl} \Omega_{kl} \right), 0 \right] \tag{2.41}$$

$$\begin{aligned}
\rho\widehat{\overline{u_i u_j}} &= c_1\frac{\mu_t k}{\tilde{\varepsilon}}\left(S_{ik}S_{kj}-\frac{1}{3}S_{kl}S_{kl}\delta_{ij}\right)\\
&+c_2\frac{\mu_t k}{\tilde{\varepsilon}}\left(\Omega_{ik}S_{kj}+\Omega_{jk}S_{ki}\right)\\
&+c_3\frac{\mu_t k}{\tilde{\varepsilon}}\left(\Omega_{ik}\Omega_{jk}-\frac{1}{3}\Omega_{lk}\Omega_{lk}\delta_{ij}\right)\\
&+c_4\frac{\mu_t k^2}{\tilde{\varepsilon}^2}\left(S_{ki}\Omega_{lj}+S_{kj}\Omega_{li}\right)S_{kl}\\
&+c_5\frac{\mu_t k^2}{\tilde{\varepsilon}^2}\left(\Omega_{il}\Omega_{lm}S_{mj}+S_{il}\Omega_{lm}\Omega_{mj}-\frac{2}{3}S_{lm}\Omega_{mn}\Omega_{nl}\delta_{ij}\right)\\
&+\frac{\mu_t k^2}{\tilde{\varepsilon}^2}\max\left[\left(c_6S_{kl}S_{kl}+c_7\Omega_{kl}\Omega_{kl}\right),0\right] \qquad (2.42)
\end{aligned}$$

Following this treatment, the turbulence energy production can be written:

$$\begin{aligned}
P_k &= -\rho\overline{u_i u_j}\frac{\partial U_i}{\partial x_j}\\
&= \left(\mu_t' S_{ij}-\rho\widehat{\overline{u_i u_j}}\right)\frac{\partial U_i}{\partial x_j} \qquad (2.43)
\end{aligned}$$

The Craft *et al*. model was developed with reference to flow in curved channels, through a rotating pipe, transitional flow over a flat plate, impinging jet flow and flow over a turbine blade [34]. The model has since been applied to abrupt pipe expansions [67], flow through ribbed passages [68], flow over a square cylinder adjacent to a wall, through a 10° plane diffuser, through a square-section U-bend and over a three-dimensional simplified car body [35]. The recent studies by Robinson in a plane diffuser concluded that the model was able to predict smooth wall separation and reattachment in an adverse pressure gradient. For flow through the U-bend which involves strong flow curvature and streamwise vorticity, the predicted velocity profiles were in good agreement with experiments (in fact, as good as the more sophisticated cubic differential stress model of Craft *et al*. [69]). However, for flow over the "Ahmed" car body, the model predicted boundary layer separation over the 25° rear slant whereas experiments (and a linear $k-\varepsilon$ model) indicated that the flow was attached. This discrepancy is discussed in greater detail in Chapter 7.

2.4 "Standard" Wall Functions

In the following section and in later discussions it is necessary to distinguish between the relatively simple log-law based wall functions and the new numerical wall function. To make this distinction clear, all the wall functions which prescribe log-law velocity and temperature profiles within the near-wall cell are called "standard" treatments. The section begins by identifying some common features of the standard wall functions which are tested in the current work, before proceeding to discuss each wall function in more detail. Implementation of the wall functions into the two codes, TEAM and STREAM, are discussed in more detail in Chapter 3.

2.4.1 Common Features

All of the standard wall functions presented below (Sections 2.4.2 to 2.4.5) follow the same functional form. Each involves the modification of the discretized transport equations for momentum, kinetic energy and dissipation rate in the near-wall cell to account for the presence of the wall. For a description of the near-wall cell notation (e.g. locations of nodes P and N) see Figure 2.1.

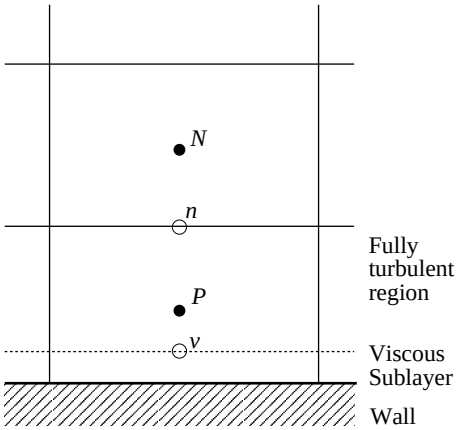

Figure 2.1: Cell notation used by standard wall functions.

Momentum

All of the standard wall functions make use of the log-law for determining the wall shear stress, τ_{wall}, using the velocity scale $\left(c_\mu^{1/4}k^{1/2}\right)$:

$$\begin{aligned} U^+ &= \frac{1}{\kappa}\ln(Ey^+) \\ \frac{c_\mu^{1/4}k^{1/2}U}{\tau_{wall}/\rho} &= \frac{1}{\kappa}\ln\left(\frac{Ec_\mu^{1/4}k^{1/2}y}{\nu}\right) \end{aligned} \tag{2.44}$$

which can be rearranged as:

$$\tau_{wall} = \frac{\rho\kappa c_\mu^{1/4}k^{1/2}U}{\ln\left(Ec_\mu^{1/4}k^{1/2}y/\nu\right)} \tag{2.45}$$

In some wall functions k is evaluated at the near-wall node, denoted k_P, and in others, at the edge of the viscous sublayer, k_v. The above conditions apply if the near-wall node is within the fully-turbulent region, which is defined as $y^+ > 11.6$. If the viscous sublayer is large in comparison to the width of the near-wall cell and $y^+ < 11.6$, the linear-law should be used:

$$U^+ = y^+ \tag{2.46}$$

which gives the following expression for the wall shear stress:

$$\tau_{wall} = \mu \frac{U}{y} \tag{2.47}$$

In the spinning-disc case examined later, the wall is rotating at an angular velocity $W_{wall} = \Omega r$. Using a stationary reference frame, the dimensionless tangential velocity is therefore given by:

$$W^+ = \frac{W - W_{wall}}{W_\tau} \tag{2.48}$$

Analogous expressions to Equations (2.45) and (2.47) can be defined for the wall shear stress in the tangential direction.

Turbulent Kinetic Energy

The transport equation for k is solved for the near-wall nodes (node P in Figure 2.1) but since production, P_k, and dissipation, ε, are expected to change rapidly across the near-wall region, it is not suitable to use values of P_k and ε evaluated at the centre of the cell. Instead, values of P_k and ε are substituted with cell-averaged $\overline{P_k}$ and $\overline{\varepsilon}$ terms which take into account the changes in turbulence quantities across the near-wall cell. These averaged quantities are approximated differently in different wall functions and it is principally through changes in the assumed profiles of turbulent stress ($\tau = -\rho\overline{u_i u_j}$) and k, used in $\overline{P_k}$ and $\overline{\varepsilon}$, that improvements in the standard wall functions are achieved.

The wall functions, presented below, all describe an averaged production term due to shear stress which is denoted $\overline{P_{kuv}}$. In impinging, separating or reattaching flows the normal stress contribution to k-production is significant and so it is inadvisable to use only the shear stress contribution. In the impinging jet and spinning disc calculations, described later, a normal stress contribution has therefore been included in $\overline{P_k}$. This has been calculated based on the normal stress at the near-wall node and the strain-rate across the cell (based on the velocity interpolated to the cell boundaries). For a two-dimensional Cartesian grid arrangement the cell-averaged production is therefore given by:

$$\overline{P_k} = \overline{P_{kuv}} - \rho\overline{uu}\frac{\partial U}{\partial x} - \rho\overline{vv}\frac{\partial V}{\partial y} \tag{2.49}$$

In Chapter 5 the effects of neglecting the normal stress contribution to $\overline{P_k}$ on heat transfer predictions for the impinging jet are discussed (see Figures 5.39 and 5.42).

Dissipation Rate

The transport equation for ε is not solved at the near-wall nodes in the standard wall functions considered here, but instead the value of ε_P is prescribed from equilibrium length scale assumptions. The

equilibrium length scale is given by:

$$l_m = c_\mu^{3/4} \frac{k^{3/2}}{\varepsilon} = \kappa y \tag{2.50}$$

and hence the dissipation rate at the near-wall node is prescribed as:

$$\varepsilon_P = \frac{c_\mu^{3/4} k_P^{3/2}}{\kappa y_P} \tag{2.51}$$

Temperature

For calculations involving heat transfer, the wall temperature is calculated using the log-law:

$$T^+ = \frac{1}{\kappa_h} \ln\left(y^+\right) + c_h \tag{2.52}$$

which can be rearranged to give:

$$T^+ = \sigma_t \left(U^+ + P\right) \tag{2.53}$$

where P is the function of Jayatilleke [44], σ_t is the turbulent Prandtl number and the dimensionless temperature, T^+, is given by:

$$T^+ = \frac{(T_{wall} - T)}{T_\tau} \qquad\qquad T_\tau = \frac{q_{wall}}{\rho c_p U_\tau} \tag{2.54}$$

This can be rearranged into an expression for either the wall temperature, T_{wall}:

$$T_{wall} = T_P + \frac{q_{wall} \sigma_t \left(U^+ + P\right)}{\rho c_p c_\mu^{1/4} k_P^{1/2}} \tag{2.55}$$

or the wall heat flux, q_{wall}:

$$q_{wall} = \frac{\rho c_p c_\mu^{1/4} k_p^{1/2} \left(T_{wall} - T_P\right)}{\sigma_t \left(U^+ + P\right)} \tag{2.56}$$

If the near-wall node is within the viscous sublayer, defined as $y^+ < 11.6$, Fourier’s heat conduction law is applied instead of the log-law:

$$T^+ = y^+ \sigma \tag{2.57}$$

where σ is the molecular Prandtl number ($\sigma = \mu c_p / \lambda$). This can be rearranged for wall temperature, T_{wall}:

$$T_{wall} = T + \frac{q_{wall}}{\lambda} y \tag{2.58}$$

or wall heat flux, q_{wall}:

$$q_{wall} = \lambda \frac{(T_{wall} - T)}{y} \tag{2.59}$$

2.4.2 Launder & Spalding (TEAM)

The original TEAM code used the wall function of Launder & Spalding [48] (see also the TEAM manual [70]). This calculates the wall shear stress from the log-law with properties evaluated at the near-wall node P:

$$\frac{c_\mu^{1/4} k_P^{1/2} U_P}{\tau_{wall}/\rho} = \frac{1}{\kappa} \ln\left(\frac{E c_\mu^{1/4} k_P^{1/2} y_P}{\nu}\right) \tag{2.60}$$

with constants $\kappa = 0.42$ and $E = 9.79$. The average production of k due to shear stress is calculated assuming a constant shear stress across the whole of the near-wall cell ($\tau = \tau_{wall}$) including viscous sublayer, and the strain-rate used in the cell-averaged production term is simply taken from the nodal value of velocity ($\partial U/\partial y = U_P/y_P$):

$$\overline{P_{kuv}} = \frac{1}{y_n}\int_0^{y_n} -\rho\overline{uv}\frac{\partial U}{\partial y}\mathrm{d}y = \tau_{wall}\frac{U_P}{y_P} \tag{2.61}$$

Likewise, the average dissipation rate is found from assuming that $-\rho\overline{uv} = \tau_{wall}$ and $\partial U/\partial y = U_P/y_P$:

$$-\rho\overline{uv} = \tau_{wall} = \mu_t \frac{\partial U}{\partial y} \tag{2.62}$$

$$\frac{\tau_{wall}}{\rho} = c_\mu \frac{k^2}{\varepsilon}\frac{U_P}{y_P} \tag{2.63}$$

and substituting in $U^+ = \rho c_\mu^{1/4} k_P^{1/2} U/\tau_{wall}$:

$$\overline{\varepsilon} = \frac{c_\mu^{3/4} k_P^{3/2} U_P^+}{y_P} \tag{2.64}$$

2.4.3 Simplified Chieng & Launder (SCL)

In the Simplified Chieng & Launder (SCL) wall function, the wall shear stress is evaluated as previously with the original TEAM wall function. For the average production, in the fully turbulent region, the turbulent shear stress is assumed to be constant and equal to the wall shear stress while in the viscous sublayer the turbulent stress is assumed to be zero (see Figure 2.2). The strain rate ($\partial U/\partial y$) is determined from differentiating the log-law.

$$\overline{P_{kuv}} = \frac{1}{y_n}\int_{y_v}^{y_n} \tau_{wall}\frac{\tau_{wall}}{\kappa c_\mu^{1/4}\rho k_P^{1/2} y}\mathrm{d}y = \frac{\tau_{wall}^2}{\kappa c_\mu^{1/4}\rho k_P^{1/2} y_n}\ln\left(\frac{y_n}{y_v}\right) \tag{2.65}$$

where the sublayer thickness, y_v, is found from assuming a constant sublayer Reynolds number, ($R_v = k_P^{1/2} y_v/\nu = 20$).

The average dissipation rate is obtained by assuming ε to be constant in the viscous sublayer and equal to its wall limiting value, such that k increases quadratically across the viscous sublayer. In the

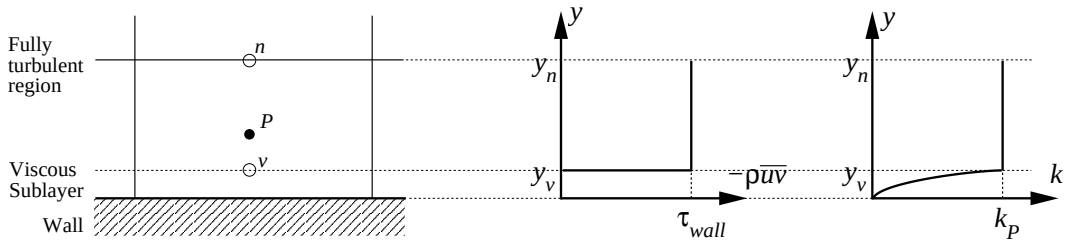

Figure 2.2: Simplified Chieng & Launder wall function: assumed profiles of turbulent shear stress $(-\rho\overline{uv})$ and turbulent kinetic energy (k) across the near-wall cell.

turbulent region ε varies according to the equilibrium length scale $\left(k^{3/2}/\varepsilon = c_l y\right)$ and the turbulent kinetic energy is assumed to be constant outside the sublayer $(k = k_P)$.

$$\overline{\varepsilon} = \frac{1}{y_n}\left(y_v \frac{2\nu k_P}{y_v^2} + \int_{y_v}^{y_n} \frac{k_P^{3/2}}{c_l y}\mathrm{d}y\right) = \frac{1}{y_n}\left[\frac{2k_P^{3/2}}{k_P^{1/2} y_v/\nu} + \frac{k_P^{3/2}}{c_l}\ln\left(\frac{y_n}{y_v}\right)\right] \tag{2.66}$$

2.4.4 Chieng & Launder (CL)

The Chieng & Launder wall function [49] accounts for variations in turbulent stress $(-\rho\overline{uv})$ and kinetic energy across the near-wall cell. The log-law is defined using k extrapolated to the edge of the viscous sublayer (k_v) in order to make the value of τ_{wall} less dependent upon the physical location of the near-wall node y_P:

$$\frac{c_\mu^{1/4} k_v^{1/2} U_P}{\tau_{wall}/\rho} = \frac{1}{\kappa}\ln\left(\frac{E c_\mu^{1/4} k_v^{1/2} y_P}{\nu}\right) \tag{2.67}$$

where the sublayer thickness, y_v, is determined from $y_v k_v^{1/2}/\nu = 20$, the integration constant is given by $E = 9.79$ and k_v is obtained by a fitting a straight-line through values of k at the two near-wall nodes, P and N (shown in Figure 2.1). To calculate $\overline{P_{kuv}}$, the turbulent stress in the viscous sublayer is assumed to be zero and in the fully turbulent region the stress is assumed to vary linearly with wall distance (see Figure 2.3). The velocity gradient $(\partial U/\partial y)$ is calculated from the log-law as previously:

$$\overline{P_{kuv}} = \frac{1}{y_n}\int_{y_v}^{y_n}\left[\tau_{wall} + \frac{(\tau_n - \tau_{wall})}{y_n} y\right]\frac{\tau_{wall}}{\kappa c_\mu^{1/4}\rho k_v^{1/2}}\frac{1}{y}\mathrm{d}y \tag{2.68}$$

$$= \frac{\tau_{wall}^2}{\kappa c_\mu^{1/4}\rho k_v^{1/2} y_n}\ln\left(\frac{y_n}{y_v}\right) + \frac{\tau_{wall}(\tau_n - \tau_{wall})}{\kappa c_\mu^{1/4}\rho k_v^{1/2} y_n^2}(y_n - y_v) \tag{2.69}$$

For the purpose of evaluating ε, k is assumed to vary quadratically in the viscous sublayer and linearly in the fully turbulent region. The cell-averaged dissipation rate is evaluated using the same assumptions as used with the SCL wall function, but with a linear interpolation for k in the fully turbulent

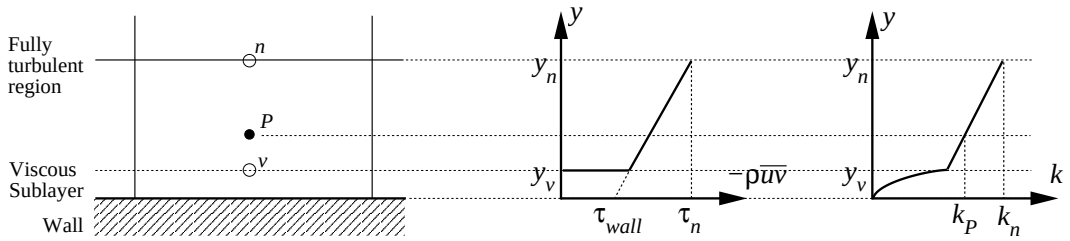

Figure 2.3: Chieng & Launder wall function: assumed profiles of turbulent shear stress $(-\rho\overline{uv})$ and turbulent kinetic energy (k) across the near-wall cell.

region:

$$\overline{\varepsilon} = \frac{1}{y_n}\left(y_v\frac{2\nu k_v}{y_v^2} + \int_{y_v}^{y_n}\frac{1}{c_l y}\left[k_n - \frac{(k_n - k_P)}{y_n - y_P}(y_n - y)\right]^{3/2}\mathrm{d}y\right) \tag{2.70}$$

The above integration is performed numerically. The turbulent kinetic energy evaluated at the northern edge of the cell, k_n, is obtained by linear interpolation between the two neighbouring nodes P and N. Following the expression for wall shear stress, τ_{wall}, the wall temperature is based on k_v rather than k_P to reduce the dependence on the position of node P:

$$T_{wall} = T_P + \frac{q_{wall}T^+}{\rho c_p c_\mu^{1/4} k_v^{1/2}} \tag{2.71}$$

where T^+ is evaluated using U^+ evaluated with k_v as for the wall shear stress expression.

2.4.5 Johnson & Launder (JL)

The Johnson & Launder wall function [50] extends the Chieng & Launder wall function by accounting for variation in the sublayer thickness, y_v. Johnson & Launder noted that if the magnitude of the shear stress falls rapidly with distance from the wall (e.g. in highly accelerated boundary layers) the thickness of the sublayer is increased beyond that which would be predicted from a constant sublayer Reynolds number, R_v. Conversely in the reattachment region of a backward step there is low wall shear stress but high shear stress and turbulence energy a short distance away from the wall. The modification proposed by Johnson & Launder is to make the sublayer Reynolds number a function of the near-wall gradient of k such that, if there is a diffusion of energy towards the wall, then the dimensionless thickness of the sublayer is reduced. This is implemented by introducing a variable sublayer Reynolds number, R_v:

$$R_v = \frac{k_v^{1/2} y_v}{\nu} = \frac{20}{1 + 3.1\lambda} \qquad \lambda = \frac{k_v - k_{wall}}{k_v} \tag{2.72}$$

where k_{wall} and k_v are extrapolated from k_P and k_n. At the edge of the sublayer $(y = y_v)$, both the log-law and the linear relationship between U^+ and y^+ can be applied (Equations 1.11 and 1.14). If

these two expressions are equated it can be shown that the integration "constant", E, in the log-law is not in fact a constant as it has been assumed up to this point, but a function given by:

$$E = \frac{\exp\left(c_\mu^{1/4}\kappa R_v\right)}{c_\mu^{1/4} R_v} \tag{2.73}$$

The Johnson & Launder wall function therefore consists of two modifications to the CL wall function: variable R_v and E.

2.4.6 Chieng & Launder Modifications

Two modifications to the Chieng & Launder wall function were tested during the course of the current work to try to reduce the sensitivity of the wall function to changes in the near-wall cell size and to improve its overall performance. In the first modification, the normal stresses were assumed to vary linearly across the fully-turbulent region of the near-wall cell when calculating the cell-average production term $\overline{P_k}$. This is a simple continuation of the approach adopted by Chieng & Launder for the shear stress variation across the cell. In the second modification, the Reynolds stresses were no longer assumed to be zero across the viscous sublayer, but instead were assumed to follow their wall-limiting behaviour (see Section 1.3). This introduces additional terms into the expression for $\overline{P_k}$. The performance of these two modifications are discussed with reference to the impinging jet flow in Chapter 5. A further modification, for which results are not shown, assumed that the length scale varies linearly across the two wall-adjacent cells in order to specify the value of the dissipation rate at the near-wall node, ε_P. This was proposed in order to reduce the sensitivity of the wall function to the size of the near-wall control volume in flows where the turbulence length scale does not follow the equilibrium length-scale variation $\left(k^{3/2}/\varepsilon = c_l y\right)$. However, it was found in the impinging jet flow that this modification introduced stability problems.

2.4.7 NLEVM Implementation

The Craft *et al*. NLEVM uses strain-rates evaluated at the near-wall node, P, to calculate the c_μ-function and the additional non-linear stress components, $\mu_t^{'}$ and $\widehat{\overline{u_i u_j}}$ in Equations (2.41) and (2.42). To be entirely consistent with standard wall functions, the strain-rate $(\partial U/\partial y)$ at node P should be obtained by differentiating the log-law:

$$\frac{\partial U}{\partial y} = \frac{\tau_{wall}}{\kappa c_\mu^{1/4} \rho k_P^{1/2} y} \tag{2.74}$$

In practice, however, using the above expression for $\partial U/\partial y$ in the non-linear terms was found to worsen the predictions of the wall functions in the impinging jet flow (see Figure 5.45 for the Chieng & Launder wall function results). All the calculations discussed in Chapters 5 to 7 assume a linear velocity profile across the cell for the strain-rate at the node used in the NLEVM terms.